

Soot climate forcing via snow and ice albedos

James Hansen and Larissa Nazarenko
PNAS vol. 101 no.2 423 - 428

Presentation : Zheng Lu

Objective

Intergovernmental Panel on Climate Change estimates the climate forcing for fossil fuel black carbon (BC) aerosol as 0.2W/m^2 (2001). But Many scientists argue that many effects are not considered. So they want to estimate magnitude of one component: BC's effect on snow/ice albedo

Basic structure of this paper

1. BC amount in the snow
2. With the BC amount, they calculate the albedo change
3. They use these data to specify the plausible albedo change for equilibrium climate simulations
4. With the model output, they estimate the efficacy of snow/ice albedo forcing relative to CO₂.
5. Transient climate simulation
6. Other roles and potential implication

BC amount in snow

Definition:

BC is commonly defined in an operational sense as the absorbing component of carbonaceous aerosols

Why in snow:

Wet deposition. The snowflakes collect the aerosol in their path with a collection efficiency of 0.2 (electrostatic attraction, temperature and vapor pressure gradient between snowflakes and environment)

Distribution:

Highly variable in space and time

BC amount in snow

Location	Observed A_v , %	BC amount, ppbw
Arctic, 1980s	$\approx 90-97$	10 (low)
		30 (mean)
NH land	$\approx 88-95$	20 (low)
		60 (high)
Greenland		2 (low)
		6 (high)
Antarctica		0.2 (South Pole)
		2.5 (Ross Shelf)

table1

1. The Arctic region

BC amounts are 10 – 50 ppbw based on the snow samples in the 1980s (ref. 6)

BC emissions from Eurasia declined sharply in 1990 (ref. 20)

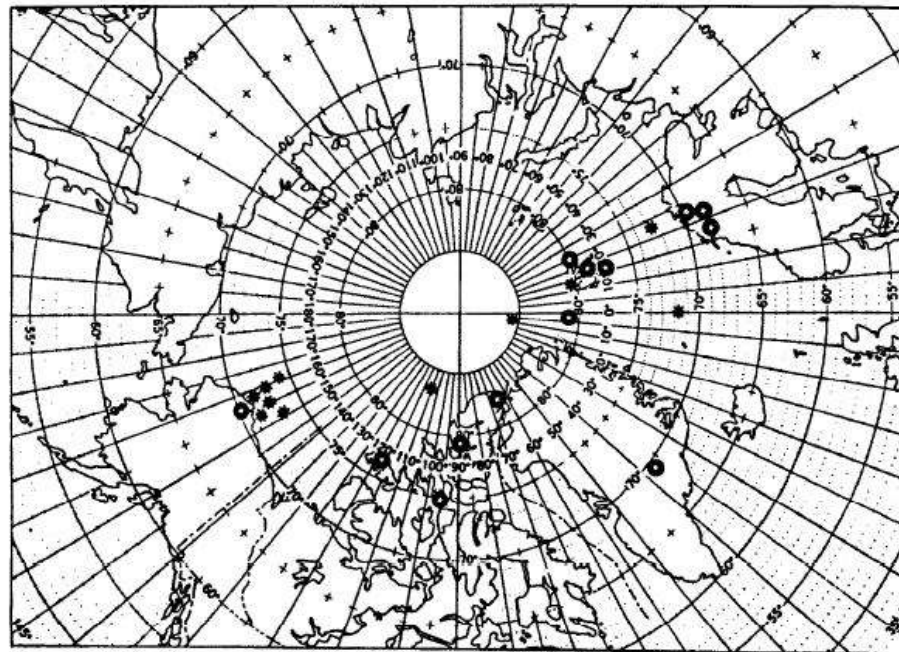
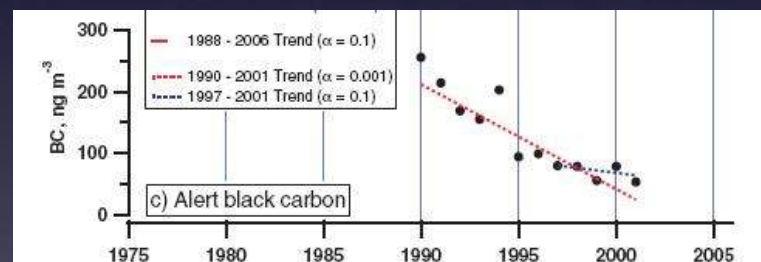
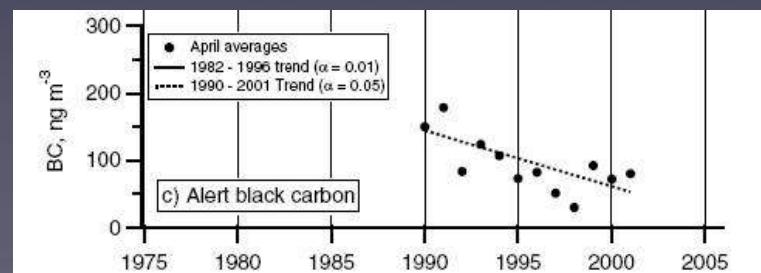


Fig. 1. Map of Arctic sampling locations for the University of Washington atmospheric (✱) aircraft samples and snowpack (✱) samples for 1983 and 1984.

Arctic sites in 1980s
Ref. 6



a



b

BC amount in Alert from
1990 to 2000
a. March
b. April
From Quinn et. Al

BC amount in snow

Location	Observed A_v , %	BC amount, ppbw
Arctic, 1980s	$\approx 90-97$	10 (low) 30 (mean)
NH land	$\approx 88-95$	20 (low) 60 (high)
Greenland		2 (low) 6 (high)
Antarctica		0.2 (South Pole) 2.5 (Ross Shelf)

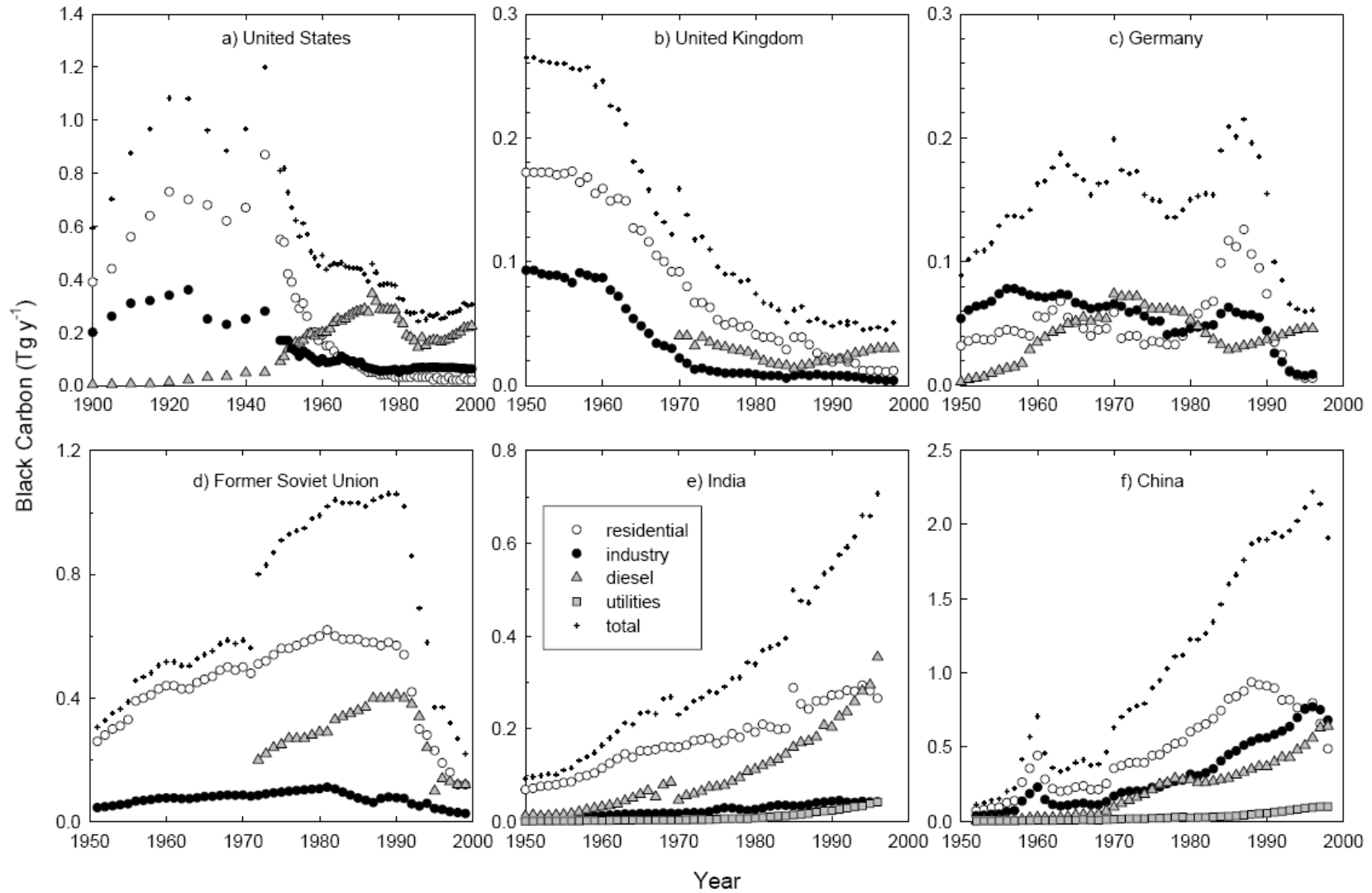
table1

2. Northern Hemisphere

Highly variable, in the range of 5 – 100ppbw

East Asia has large BC amounts, due to the largest BC sources of China and India

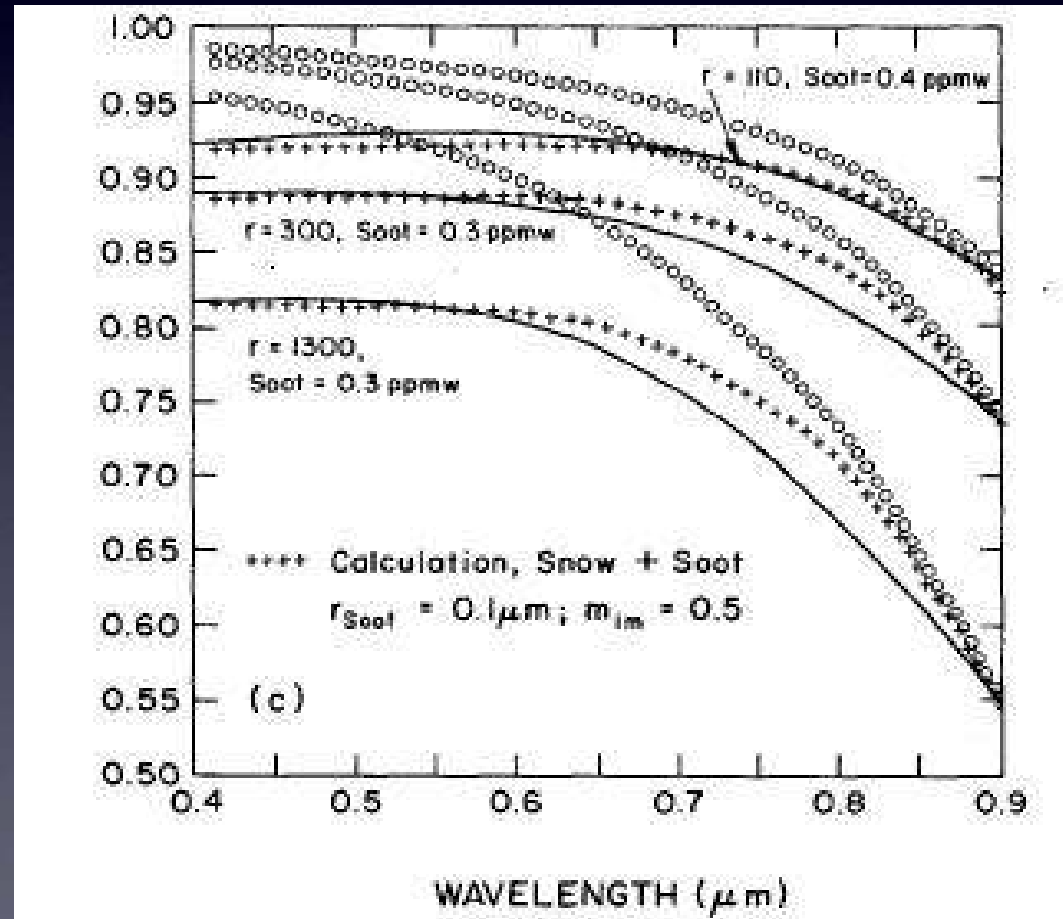
Figure 1



Ref. 20 BC emission

Albedo change

Mie scattering and multiple scattering approximation



Ref. 8

External mixture of snow and soot.

Y-axis: albedo

Circle: calculated pure snow

Line: observation (Grenfell & Maykut)

Plus: Calculated snow&soot

Soot concentration: 300ppb!

Imaginary part of soot: 0.5

Albedo change

Uncertainties:

1. If snow and BC are internal mixed, the absorption power of BC increases by a factor 1.4+
2. Soot particle shape: increases power by a factor 2+
3. Voids in the soot: increases absorption power in proportion to void fraction
4. There is large uncertainty in the optical constants of soot.

Albedo change

Table 1. Measured BC amount and calculated visible snow albedo change

Location	Observed A_v , %	BC amount, ppbw	Calculated ΔA_v , %			
			New snow		Old snow	
			Ext	Int	Ext	Int
Arctic, 1980s	≈ 90 –97	10 (low)	0.8	1.5	2.5	4.5
		30 (mean)	1.9	3.2	6.0	9.5
NH land	≈ 88 –95	20 (low)	1.5	2.5	4.5	7.7
		60 (high)	3	5	9	14
Greenland		2 (low)	0.3	0.5	0.7	1.2
		6 (high)	0.5	0.9	1.7	3.0
Antarctica		0.2 (South Pole)	.05	0.1	0.1	0.2
		2.5 (Ross Shelf)	0.3	0.5	0.8	1.5

NH, Northern Hemisphere; Ext, external mixing; Int, internal mixing.

climate simulation with specified albedo change

Table 2. Specified snow and ice albedo changes

Experiment	Arctic, %	NH land, %	Antarctica, %	Rest of SH, %
Case 1	2.5 (vis λ)	5 (vis λ)	0	1 (vis λ)
Case 2	2.5 (vis λ)	5 (vis λ)	0	0
Case 3	0	5 (all λ)	0	0
Case 4	2.5 (all λ)	0	0	0

They use multiple cases to determine the contributions of different geographical regions (implicit assumption: the response is linear for these small forcings)

Case 1 & 2: The snow albedo at $\lambda < 0.77\mu\text{m}$ is decreased 2.5% ($2.5\% \times 0.6 = 1.5\%$ spectrally averaged) in Arctic region, and by 1% at $\lambda < 0.77\mu\text{m}$ in Greenland (negligibly to the hemispheric mean response), and by 5% at $\lambda < 0.77\mu\text{m}$ ($5\% \times 0.6 = 3\%$ spectrally averaged) in the other snow-covered region in the Northern Hemisphere.

Case 3 & 4: change the albedo individually for Arctic ice and Northern Hemisphere at all wavelength solely to assure good signal/noise response

There is no albedo change in Antarctica. Case 1 has 1% albedo change in snow-covered region of Southern Hemisphere other than Antarctica (most realistic case)

climate simulation with specified albedo change

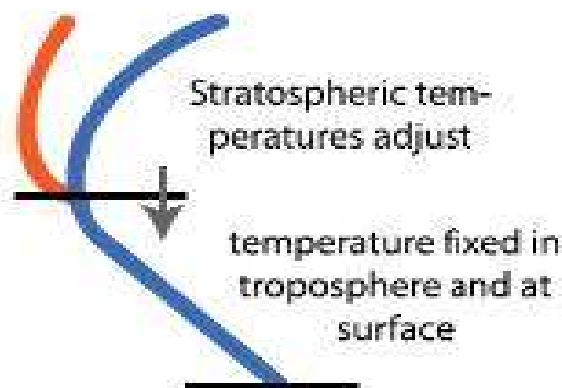
Climate Model:

Goddard Institute for Space Studies climate model

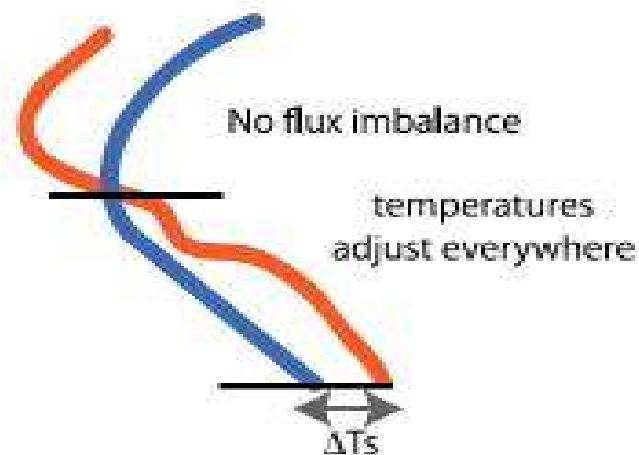
Resolution is $4^\circ \times 5^\circ$ with 18 layers. The model top is 0.1 hPa. The climate sensitivity of the model is $\approx 2.6^\circ\text{C}$ for double CO_2 .

Climate forcing: The adjusted forcing is obtained as the flux change at the top of the atmosphere after the stratospheric temperature has adjusted to the presence of the perturbation with troposphere and surface temperature fixed. Then the equilibrium response surface T_s to these forcing is calculated in the model

Stratospheric-adjusted RF

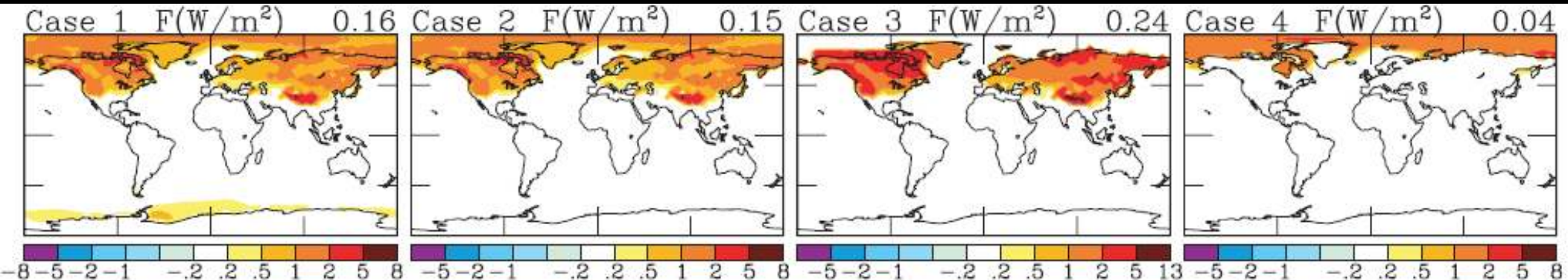


Equilibrium climate response



(IPCC 2007)

climate simulation with specified albedo change: Model output

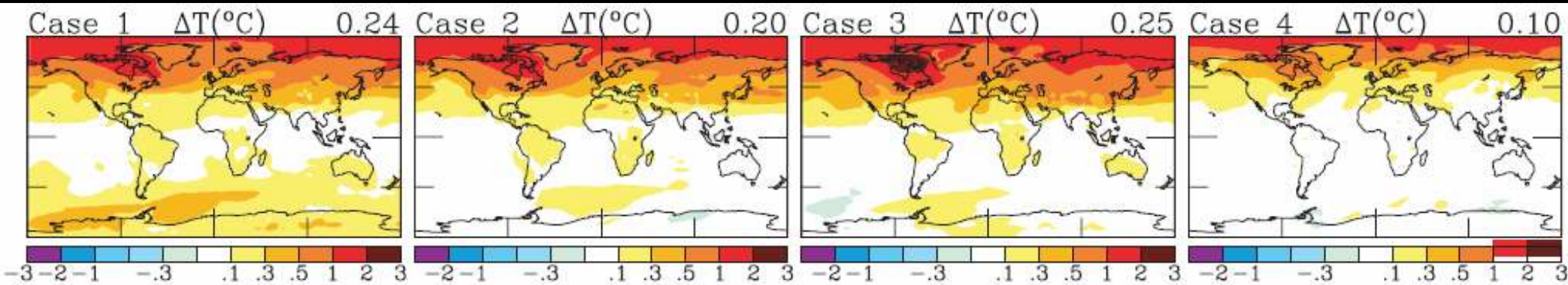


Climate forcing in W/m^2 for changes of snow and ice albedos specified in Table 2.
Numbers on the upper right are global means

1 Climate forcing

The climate forcing due to snow/ice albedo change is of the order of 1W/m^2 at middle- and high-latitude land areas in the Northern Hemisphere and over the Arctic Ocean for case 1 and 2, which have a realistic magnitude for soot effect. The mean NH forcing is $\approx 0.3\text{ W/m}^2$

climate simulation with specified albedo change: Model output



equilibrium annual-mean T_s response in $^{\circ}\text{C}$ (Lower) for changes of snow and ice albedos specified in Table 2. Numbers on the upper right are global means.

2 Equilibrium response

The annual mean response of surface temperature (T_s) is shown above. The calculated warming is unexpectedly large relative to the forcings

climate simulation with specified albedo change: Model output

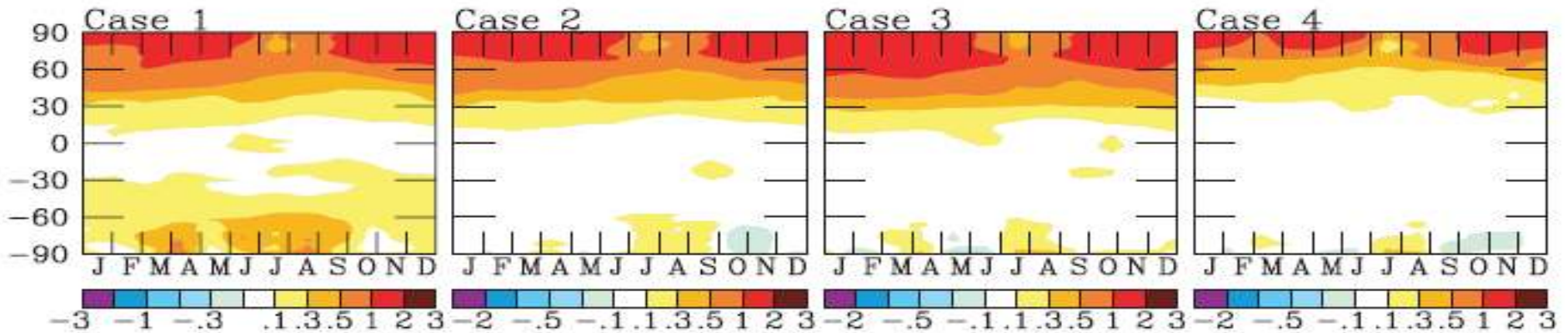


Fig. 2. Equilibrium T_s ($^{\circ}\text{C}$) response to the snow/ice albedo forcings of Fig. 1 as a function of month and latitude.

2 Equilibrium response

Fig.2 shows the calculated equilibrium T_s response as a function of month and latitude. It shows a warming at middle and high latitude that is large in winter, extends into the spring, and is minimal in summer. it is consistent with observed temperature change since 1880 (Fig.3)

Efficacy and effective forcing

Efficacy of a climate forcing is defined as the ratio of the equilibrium T_s change for that forcing to the temperature change for the same magnitude of forcing by CO₂, which is expected to be the largest anthropogenic climate forcing. (Ratio of two climate sensitivities)

They did not run the climate model for a CO₂ forcing of same magnitude, but used the assumption that the CO₂ response is proportional to the forcing.

Efficacy and effective forcing

Table 3. Climate forcings and their efficacies

Experiment	Forcing, W/m ²		Response, ΔT , °C	Efficacy		F_G W/m ²
	F_i	F_a		E_i	E_a	
2× CO ₂	4.05	3.63	2.57	1.00	1.00	3.63
Case 1	0.17	0.16	0.24	2.22	2.12	<u>0.34</u>
Case 2	0.16	0.15	0.20	1.97	1.88	0.28
Case 3	0.23	0.24	0.25	1.71	1.47	0.35
Case 4	0.04	0.04	0.10	3.94	3.53	0.14

Table 3 shows the efficacies for the snow/ice albedo forcing for the two definitions of climate forcing F_i (instantaneous), and F_a (adjusted).

For these forcings, the efficacies ≈ 2

The effective forcing is defined as $F_e = F_a E_a$. F_e provides a better measure of expected climate forcing mechanism. F_e in case 1 and 2 is $\sim 0.3 \text{ W/m}^2$ globally.

Efficacy and effective forcing

Table 3. Climate forcings and their efficacies

Experiment	Forcing, W/m ²		Response, ΔT , °C	Efficacy		F_G W/m ²
	F_I	F_a		E_I	E_a	
2× CO ₂	4.05	3.63	2.57	1.00	1.00	3.63
Case 1	0.17	0.16	0.24	2.22	2.12	0.34
Case 2	0.16	0.15	0.20	1.97	1.88	0.28
Case 3	0.23	0.24	0.25	1.71	1.47	0.35
Case 4	0.04	0.04	0.10	3.94	3.53	0.14

The variation of the efficacy from one case to another is due mainly to the latitude of the forcing.

The response to polar forcing is larger than the response to lower latitude forcing, because:

1. The ability of a high-latitude forcing to simulate snow/ice albedo feedbacks;
2. The relative stability of the atmospheric temperature profile at high latitude, which tends to confine the thermal response to the surface.

Transient Simulation

Scenario:

The transient simulation for 1880 – 2000 by using a simple soot snow/ice albedo forcing

The time dependence of the forcing is taken proportional to global mean BC amount

They take the geographical distribution of the forcing as in the case1 (with global climate forcing 0.16W/m^2). Based on the Koch/Novakov BC scenario, 83% of the 1850-2000 BC increase occurs during 1880-2000. So the forcing in the transient simulation increases by 0.83×0.16
 $\sim 0.13\text{W/m}^2$

Transient Simulation

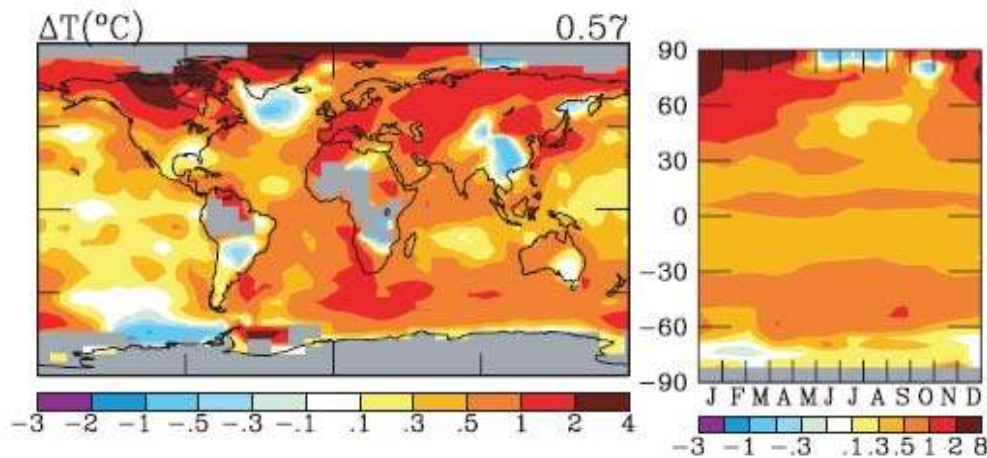


Fig. 3. Observed 1880–2002 T_s change based on adjusted meteorological station data over land (28) and sea T_s data for the ocean (29, 30).

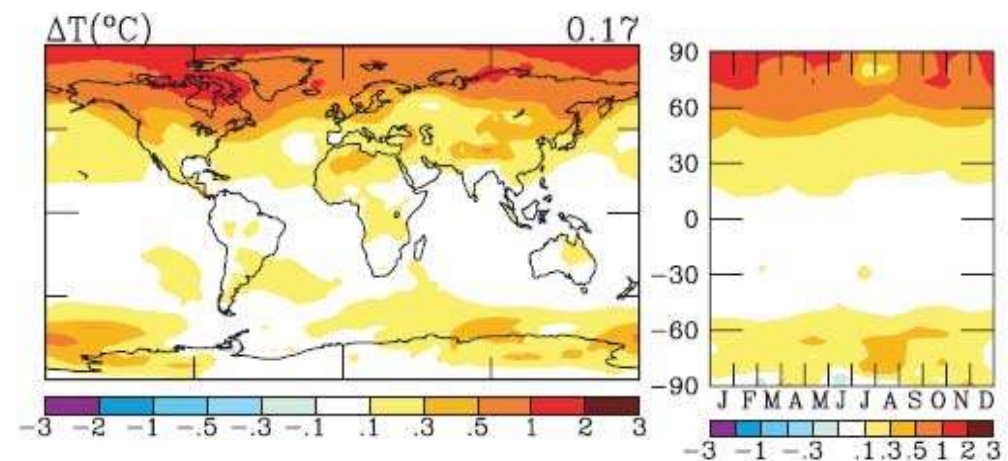


Fig. 4. Simulated 1880–2002 T_s change for the transient BC snow/ice albedo forcing that peaks in the 1990s with 83% of the case 1 forcing of Fig. 1.

The exact pattern of simulated warming has limited meaning, because of the crude spatial distribution of the forcing and the simple representation of the ocean. However the mean warming 0.17 °C is an indication of what should be expected for the assumed albedo change.

Transient Simulation

The space and seasonal features are consistent with observations. But this does not confirm the soot albedo effect. Because other forcings may have a similar impact on the pattern of climate change.

So all forcings need to be investigated one-by-one in systematic simulations and compared with observation.

Other roles and potential implication

1 Melting snow tends to retain aerosols, darkening the surface more in the winter and spring, thus increasing absorption and lengthening the melt season.

2. If the sea surface level is defined as the level of dangerous anthropogenic interference (DAI). Then reducing soot emission would have the double benefit of reducing global warming and raising the global temperature level at which DAI occurs.

Summary

1. Plausible estimates for the effect of soot on snow and ice albedos (1.5% in the Arctic and 3% in Northern Hemisphere land areas) yield a climate forcing of $+0.3 \text{ W/m}^2$ in the Northern Hemisphere.

2 Soot snow /ice albedo climate forcing has a high efficacy ≈ 2 , which is the result of positive albedo feedbacks and atmospheric stability at high latitudes.

Break for Technical Questions

Sensitivity study of the effect of increased aerosol concentrations and snow crystal shapes on the snowfall rate in the Arctic.

U. Lohmann and J. Zhang
J. Geophys. Res., Vol. 108, No. D11

Objective:

To investigate what influence anthropogenic aerosols and snow crystal shape may have on the precipitation in the Arctic with the GESIMA model.

Basic structure of this paper:

- 1) Description of model and data
- 2) Two cases studies to evaluate the model performance
- 3) Two aerosol scenarios and two different snow crystal shapes are assumed to study aerosol effect on microphysical processes and surface precipitation

Model Description

GESIMA:

3-dimensional, time-dependent, nonhydrostatic mesoscale model;

The horizontal domain: 50km*50km (25*25 grids)
resolution: 2km

The vertical domain : 9km (46 layers)
resolution: from 50m(surface) to 300m (near 9km)

Dynamical part of model is based on the conservation laws for momentum, energy, and mass

Model Description

Cloud scheme:

Cloud scheme is developed for numerical studies of cirrus and stratus clouds

Prognostic variables in the scheme: the mixing ratio of water vapor; mixing ratios and number concentrations of cloud species (cloud droplets, ice crystal, rain, and snow)

Parameterized microphysical processes are condensational growth of cloud droplets, depositional growth of ice crystals, homogeneous, heterogeneous and contact freezing of cloud droplets, autoconversion of cloud droplets, aggregation of ice crystals, accretion of ice crystals, cloud droplets and drizzle by snow, accretion of cloud droplets by rain, evaporation of cloud liquid water and rain, sublimation of ice crystals and snow, melting of ice crystals and snow and sedimentation of ice crystals, snow flakes and raindrops.

Model Description

Cloud droplet nucleation

The number of nucleated cloud droplets N_c is function of the vertical velocity w (cm s^{-1}) and the accumulation mode aerosol number concentration N_a (cm^{-3}):

$$N_c = w N_a / (w + c N_a)$$

N_a is valid for ammonium sulfate, assuming a lognormal size distribution with a mode radius of 0.05 and geometric width $\sigma=2$ at 800hPa and 273K

Model Description

Rimming process (snow collect supercooled cloud water):

The rate of change in snow mixing ratio q_s due to riming is based on the geometric sweep-out integrated over all snow size with an assumed exponential snow size distribution ($N(D) = N_{os} \exp(-\lambda D)$):

$$\left(\frac{\partial q_s}{\partial t}\right)_{riming} = \frac{\pi E_{sw} n_{os} a q_w \Gamma(3+b)}{4 \lambda_s^{(3+b)}} \left(\frac{\rho_0}{\rho}\right)^{0.5}$$

Model Description

Collection efficiency E_{sw} :

If Reynolds number is above 40 & Stokes number is between 0.06 and 0.3: accretion efficiency for aggregates

Outside this range: accretion efficiency for planar

Reynolds number $Re = UL/\nu.$

Stokes number $Stk = \frac{\tau U_o}{d_c}$

d_c is the characteristic dimension of the obstacle: Eq3&4

$$d_{pl} = 10^{-2} \sqrt{\frac{q_S \cdot 10^3 \rho}{3.8 \cdot 10^{-4} N_S}}$$

$$d_{agg} = 10^{-3} \left(\frac{q_S \cdot 10^6 \rho}{0.04 N_S} \right)^{0.714}$$

Model Description

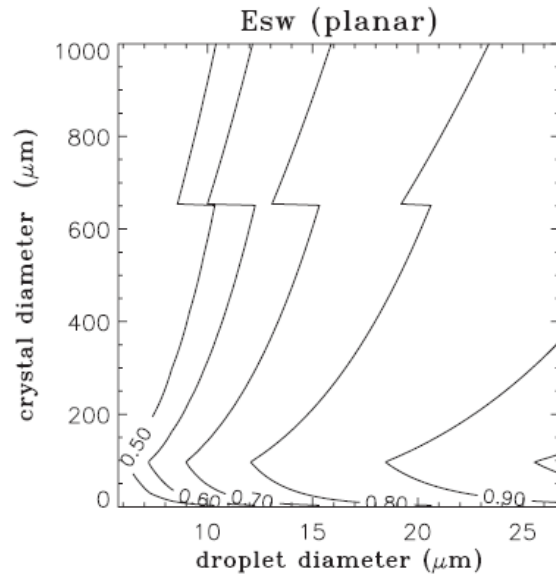


Figure 1. Collection efficiency of snow flakes with cloud droplets as a function of crystal and droplet size and for planar crystals.

Basically, the collection efficiency of larger cloud droplet and smaller snow crystal is higher

With the same water content, the planar crystal is one order of magnitude larger than aggregates, so the collection efficiency of planar crystal is smaller

Data Description

Data are from two projects: The FIRE (First ISCCP (International Satellite Cloud Climatology Project) Regional Experiment) ACE (Arctic Clouds Experiment) and SHEBA (Surface Heat Budget of the Arctic Ocean) project

Temperature, pressure and surface precipitation were obtained from an integrated SHEBA data

Potential temperature, wind speed, relative humidity (corrected) were obtained from rawinsonde data

Aerosol number concentration was measured by Condensation Particle Counter mounted on aircraft

Data Description

Adjusted IWC and LWC:

The liquid water probe can measure LWC and TWC. But the probe can also response to the IWC in a mixed-phase cloud, so they use the adjusted IWC and LWC:

$$\begin{aligned} IWC &= 1.25(TWC_{\text{mea}} - LWC_{\text{mea}}) \\ LWC &= TWC_{\text{mea}} - IWC \end{aligned}$$

IWC and r_e retrieval from radar

$$IWC = aZ^b$$

$$r_e = 0.14 \left(\frac{Z}{74 \times 10^{-6} IWC} \right)^{\frac{1}{1.9}}$$

Z is the radar reflectivity. Retrievals of effective radius may be biased toward larger ice particle sizes because the radar backscatter is proportional to the 6th moment of the size distribution

Two cases studies: 16 April

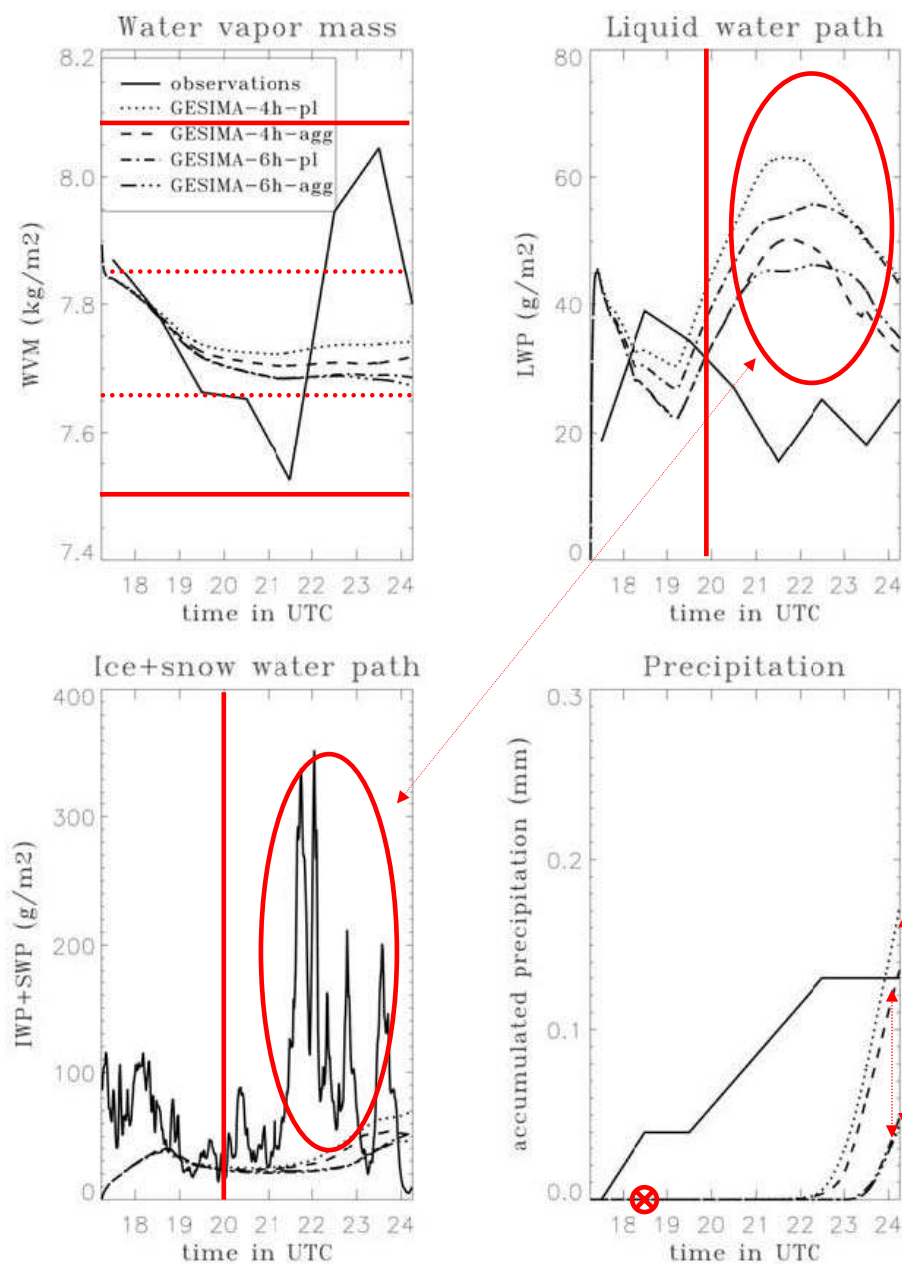
A deep, single-layer precipitating mixed-phase cloud was observed on that day

The simulated domain is initially horizontally homogeneous. A random temperature perturbation between 1200m and 6000 m with a magnitude 0.1 K was applied for the first 10 minutes of the simulation.

Nudging technique is applied to relax the model state toward observation state by adding additional term to the model equations

$$\frac{\partial X}{\partial t} = T_{ex} + \frac{(X_{obs} - X_0)}{\tau_x}$$

X represents the prognostic variable T_{ex} is the tendency calculated by model. τ_x is the nudging time scale. X_{obs} and X_0 are the observed and model calculation values of X



3. Temporal evolution of water vapor mass, liquid water path, ice and snow water path and precipitation from observations and 4 simulations with GESIMA using a 4-hour and 6-hour nudging time scale assuming planar crystals (pl) and aggregates (agg) on 16 April 1998.

1. The water vapor mass varies from 7.5 and 8.1 Kg/m². The model can't capture these variation.
2. After 2000UTC, the agreement diverges: more solid phase in observation; more liquid phase in GESIMA model
3. The observed accumulated precipitation: The model start accumulate the precipitation after 1815UTC. The differences in nudging timescale appear to be most pronounced. The difference is reduced when snow crystals are assumed to be aggregates.
4. They focus on the 4-hour nudging timescale simulations with aggregates for the remainder

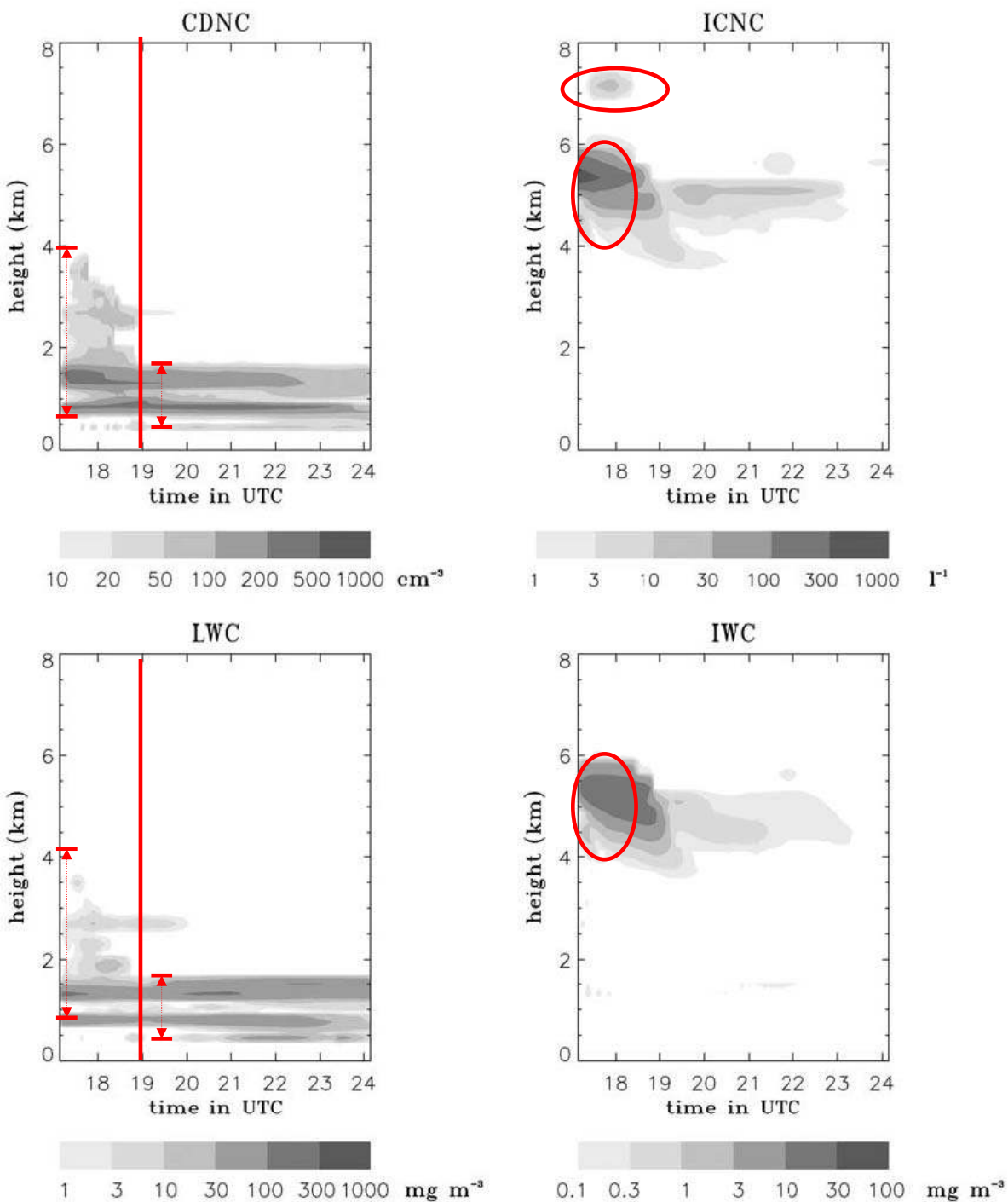


Figure 4. Temporal evolution of the simulated cloud droplet (CDNC), ice crystal (ICNC) number concentrations, liquid (LWC), and ice (IWC) water contents horizontally averaged over the cloudy part of the domain on 16 April 1998.

1. CDNC & LWC: liquid water cloud initially forms between 700m and 4000m. By 1900 UTC, the upper portion of the cloud is frozen and cloud top of the liquid cloud layer decreases down to 1700 m. The cloud becomes denser and cloud base starts to extend downward to 400 m by 1900 UTC.
2. ICNC & IWC: an altostratus layer between 4km and 6km and a thin cirrus at 7km. As snow flakes form, the ICNC and IWC decreases

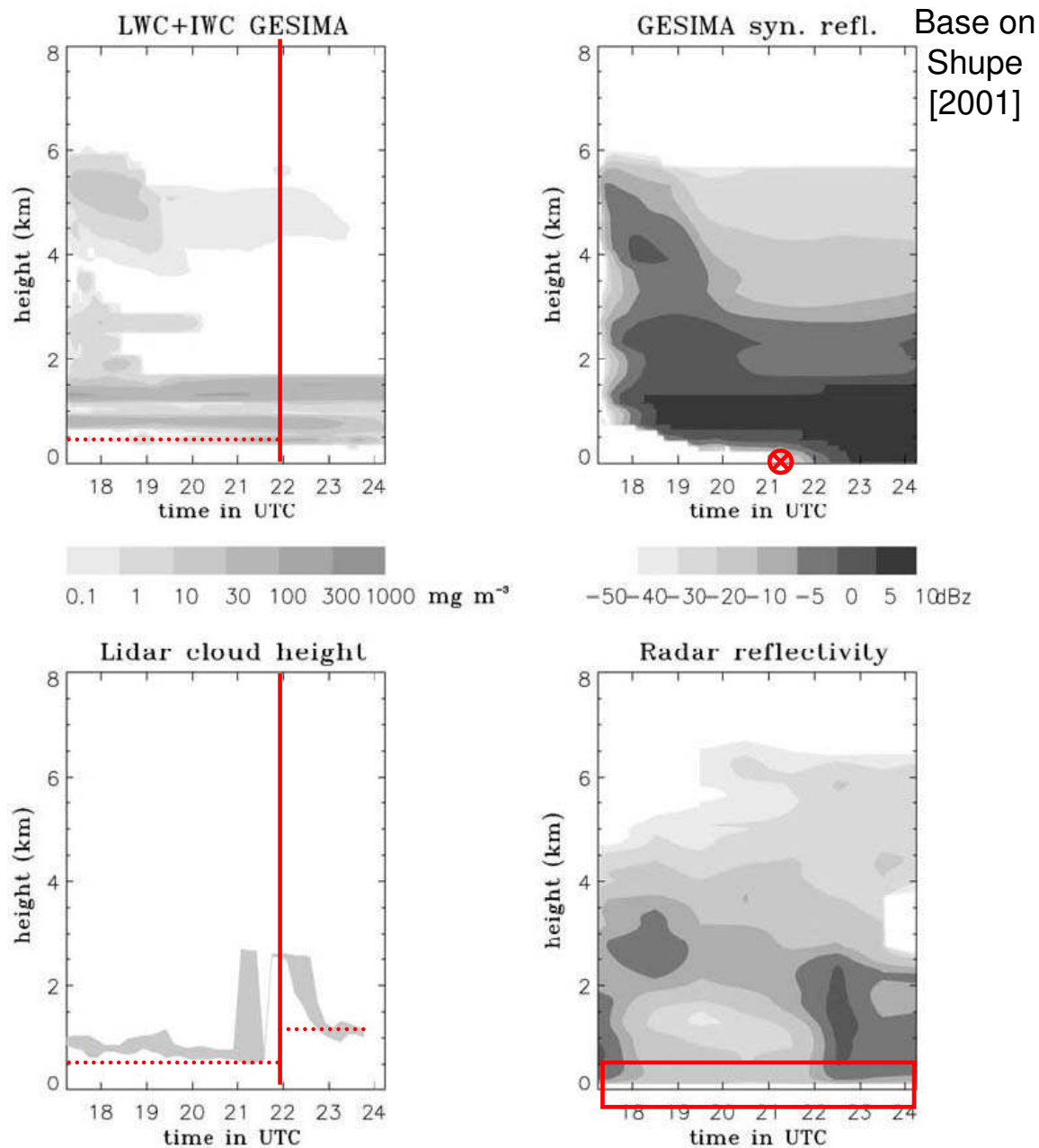


Figure 5. Temporal evolution of the domain averaged cloud altitude simulated by GESIMA as obtained from the sum of liquid and ice water content, synthetic reflectivity calculated from GESIMA, cloud base detected by lidar, and reflectivity obtained by the radar deployed on SHEBA ship on 16 April 1998.

1. The cloud base agrees with lidar measurement before 2200UTC after which lidar measures a higher cloud base than simulated.
2. The radar detects a signal down to the surface the whole time. In GESIMA it takes until 2115UTC before the precipitation reaches the surface

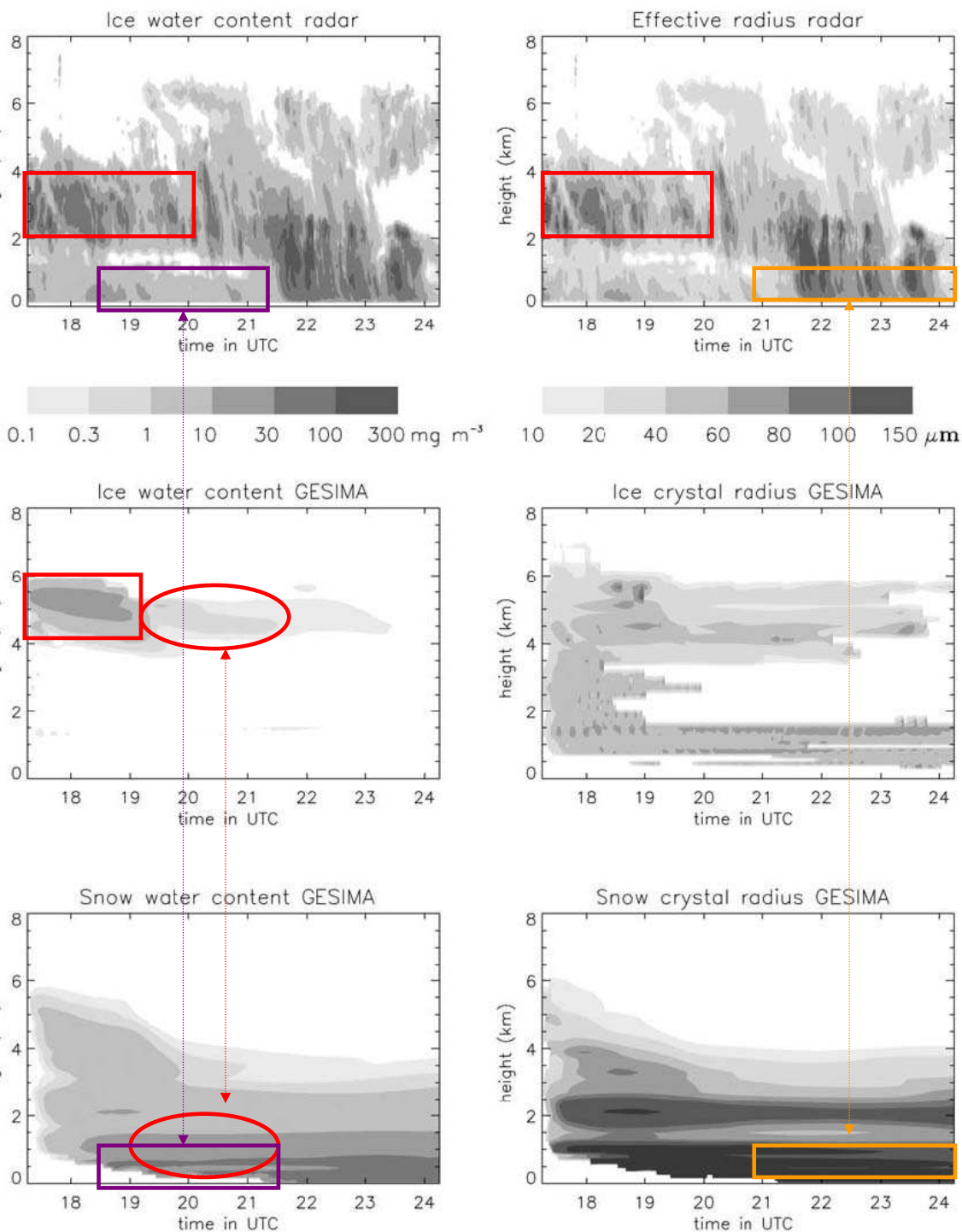


Figure 6. Temporal evolution of IWC and effective radius retrieved from radar and IWC and snow water content (SWC) and their effective radii simulated by GESIMA on 16 April 1998.

1. The observed maximum ice water content and effective radii occur initially between 2 and 4 km. In GESIMA, the IWC occurs between 4 and 6 km, and decreases with time as aggregation forms snow flakes.
2. The simulated snow water content is larger than observed below 1.5 km before 2130 UTC
3. GESIMA overestimates the snow crystal size near the surface, and underestimates the temporal variability.

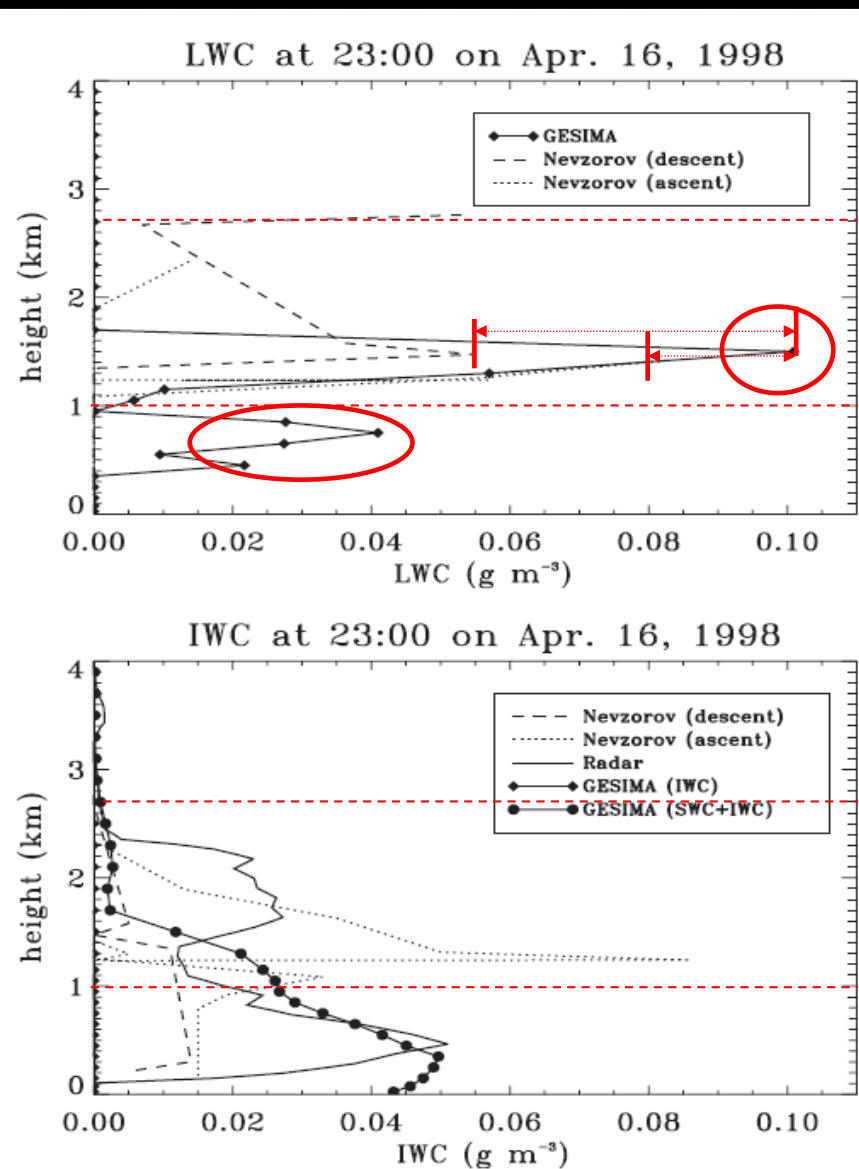


Figure 7. Vertical profiles of LWC and IWC at 2300 UTC on 16 April 1998 simulated by GESIMA and measured by aircraft and radar retrieval. The aircraft LWC and IWC were the derived ones according to equations (5) and (6) based on 10 s averaged data.

Figure 7 shows the comparison of the simulated and measured liquid and ice water content from the Canadian aircraft and the radar.

1. Mixed phase cloud exists between 1000m and 2600m
2. The simulated liquid water cloud is lower than observed with one maximum between 1 and 2 km and two secondary peaks below 1 km.
3. The LWC in GESIMA exceeds the microphysics measurements during ascent by 0.02g/m^3 , and during descent by 0.04g/m^3
4. GESIMA essentially captures the features of the observed cloud

Two cases studies: 28/29 April

The model is initialized with corrected rawinsonde data taken at 2315UTC on 28 April 1998.

Total simulation time is 7 hours. A random temperature perturbation between 2 km and 8 km with a magnitude 0.1 K was applied for the first 10 minutes of the simulation.

They still focus on the 4-hour nudging timescale simulation with aggregates.

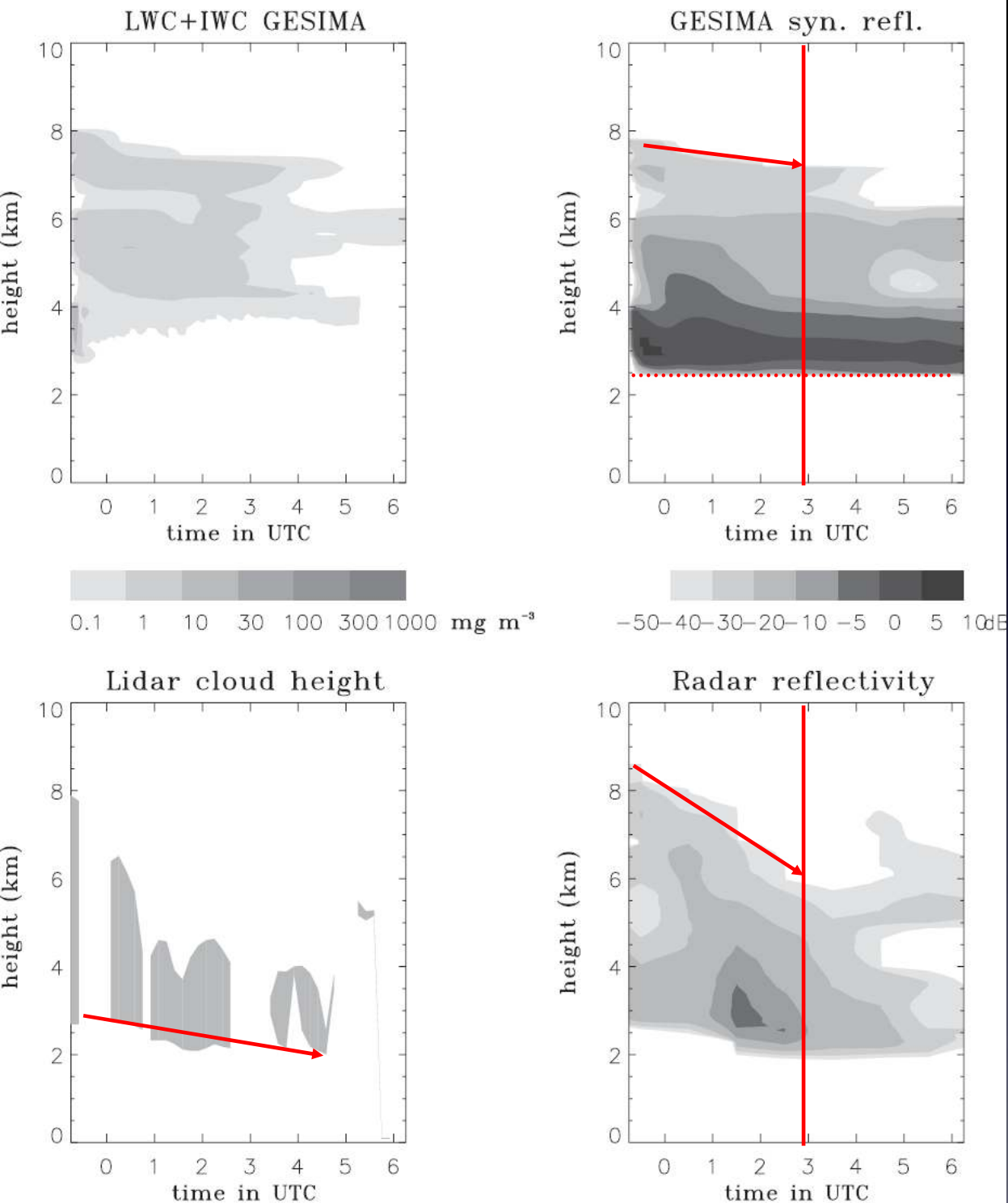


Figure 8. As in Figure 5 but for 28/29 April 1998.

1. Simulated cloud base is at 2.5km, as detected from both lidar and radar.

2. However it misses the dynamical fluctuations: occasionally observed decreases of cloud base from lidar down to 2km; The radar echo top decreases from 8km at 2315UTC to 6km at 0300UTC on 29 April, while the simulated radar echo top decreases at a slower rate.

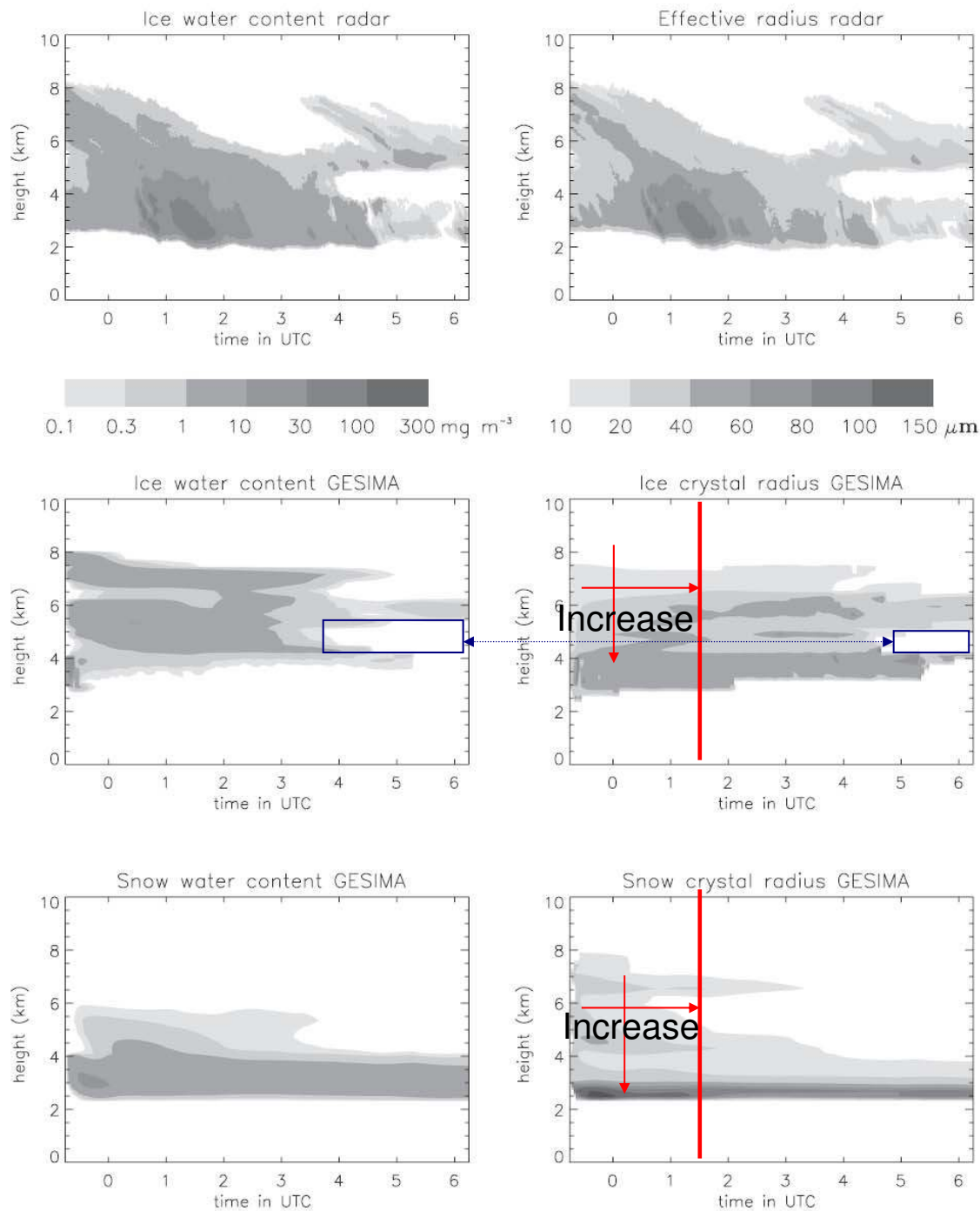


Figure 9. As in Figure 6 but for 28/29 April 1998.

1. Similar to the radar retrieval, the simulated ice crystal and snow flake effective radii and radar reflectivity increase from cloud top to cloud base and increase with time until 0130 UTC on April 29
- 2.

GESIMA also indicates the break up of the ice cloud in two distinct layers with a cloud free area between 4 and 5 km at 0400 UTC on 29 April in terms of ice water content, but the cloud free area is smaller and delayed by half an hour when evaluated in terms of effective ice crystal radius suggesting that the cloud has not completely sublimated by 0400 UTC on 29 April.

Effect of increased aerosol concentration on Precipitation

Two sensitivity experiments for the 16 April case study. For clean case: vertically uniform accumulation mode aerosol concentration of 100 cm^{-3} (AP100). For polluted case: 1000 cm^{-3} (AP1000). AP1000 is representative of a polluted episode as observed at 650m and around 4km during the 16 April case study

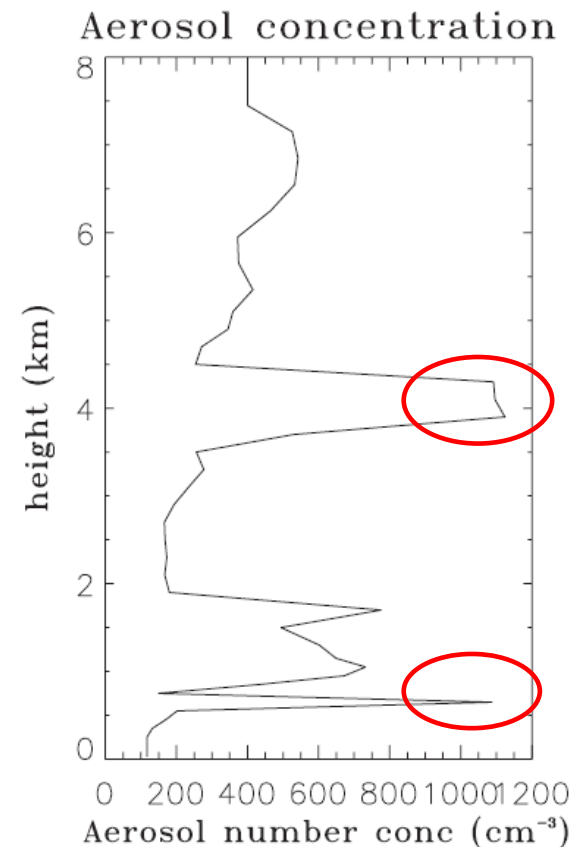


Figure 11. Vertical profile of the aerosol number concentration (cm^{-3}) from aircraft measurements on 16 April 1998.

Effect of increased aerosol concentration on Precipitation

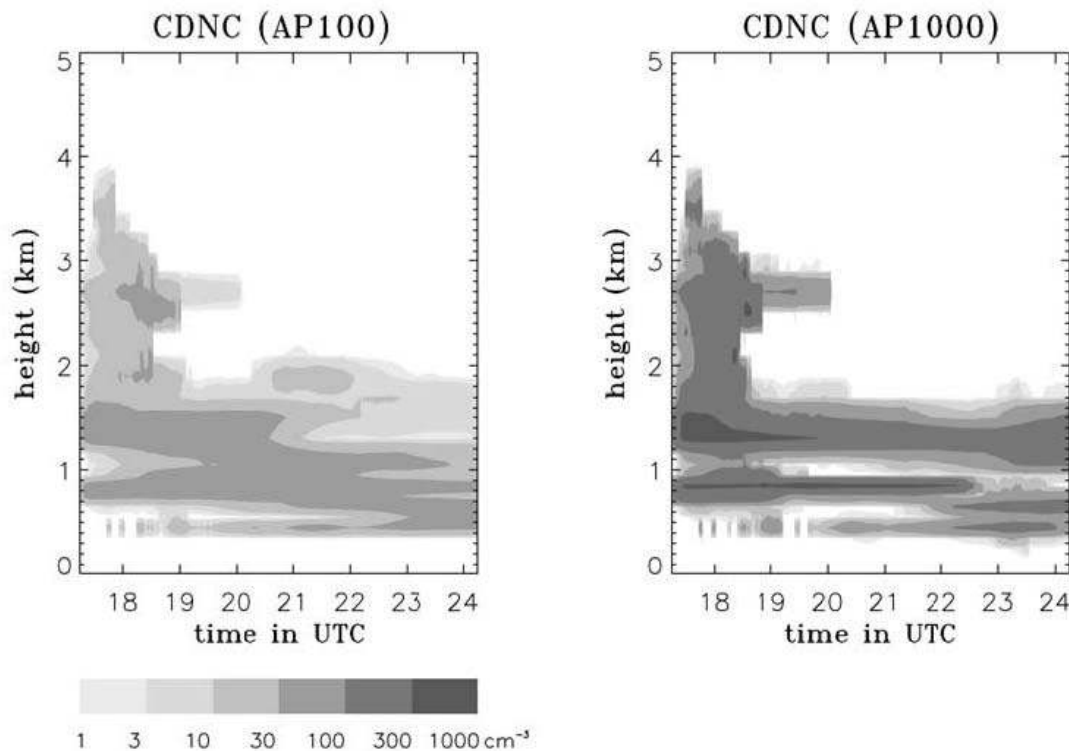
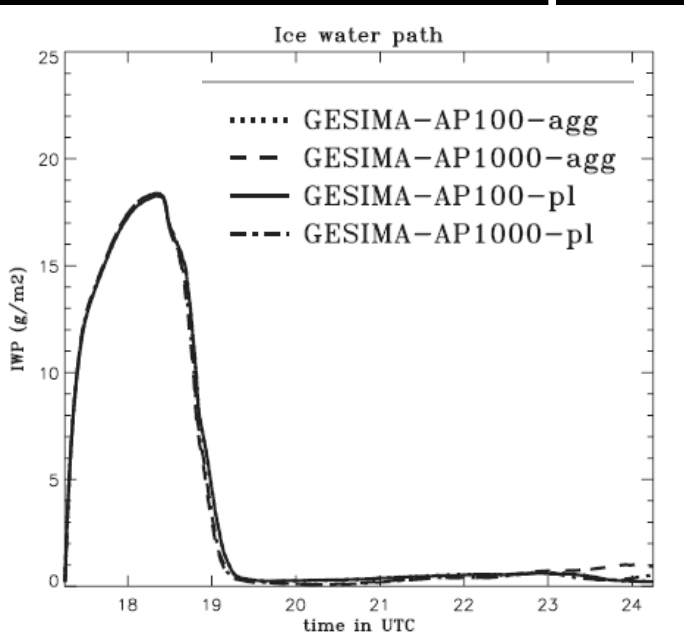


Figure 12. Temporal evolution of CDNC in the AP100 and AP1000 aerosol scenarios assuming aggregates.

1. The tenfold increase in aerosol concentration leads up to an eightfold increase in the number of cloud droplet
2. It does not influence the upper level ice cloud as ice crystal formation in GESIMA does not depend on the aerosol number concentration

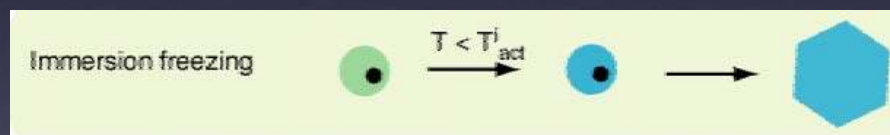
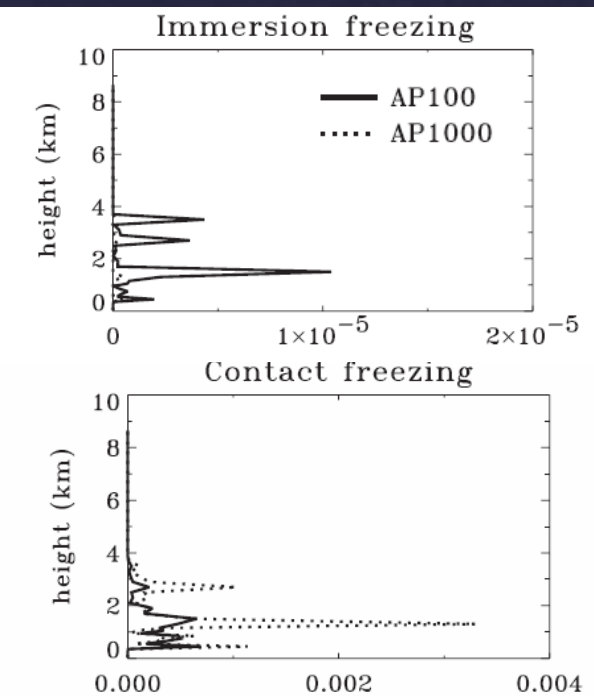
3. The clean cloud is slightly thicker after 2030UTC and does not break into two layers as the polluted cloud

Effect of increased aerosol concentration on Precipitation: ice water path

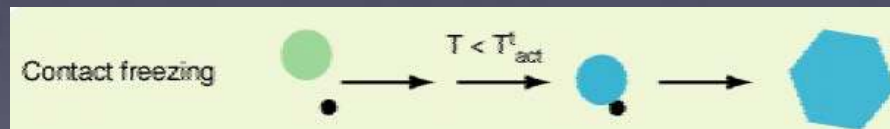


The ice water path evolution is very similar in all simulations. The slight differences are due to different nucleation freezing.

The large droplets in AP100 are more readily subject to immersion freezing while more abundant droplets in AP1000 experience more contact freezing.



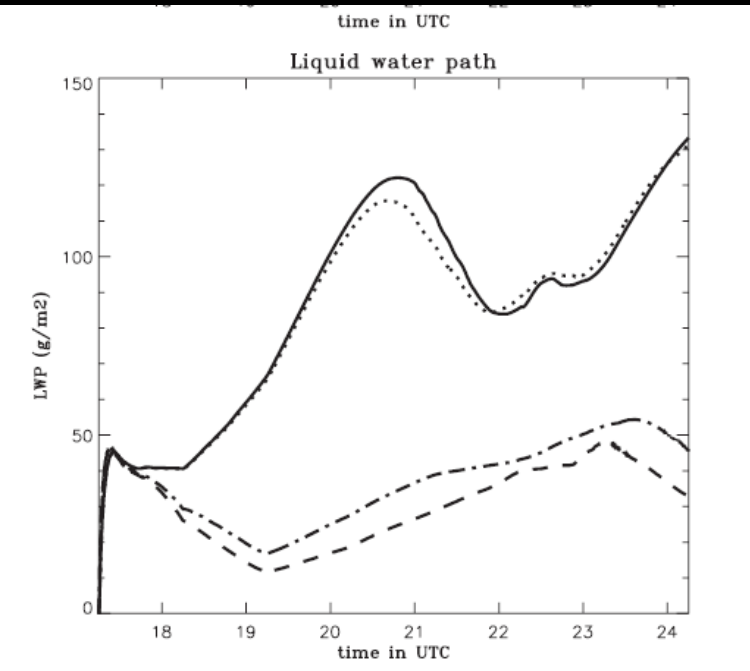
Water droplets are formed before the cooling. And afterward supercooled until they reach a crucial T where they start freezing



Refers to a freezing event resulting from a few seconds encounter between a supercooled drop and a nucleating substance

(G.Vali, 1999)

Effect of increased aerosol concentration on Precipitation: liquid water path

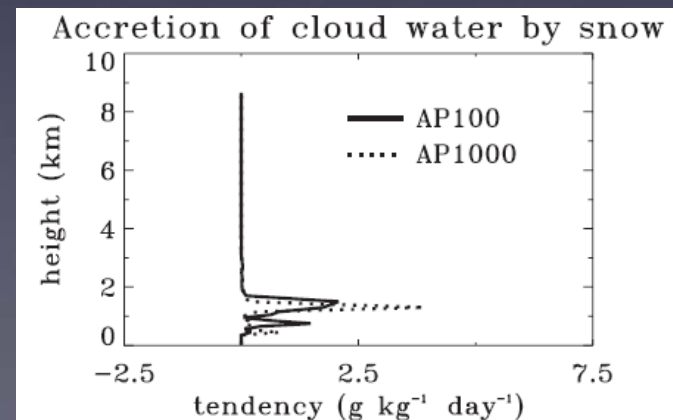


The liquid water path is roughly twice as large in AP100 as compared to AP1000 regardless of the snow crystal shape

The reduced accretion of cloud droplets by snow crystal in AP100 produces more cloud water

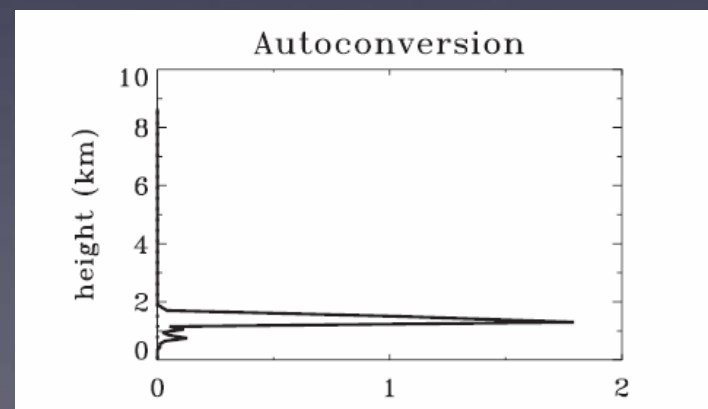
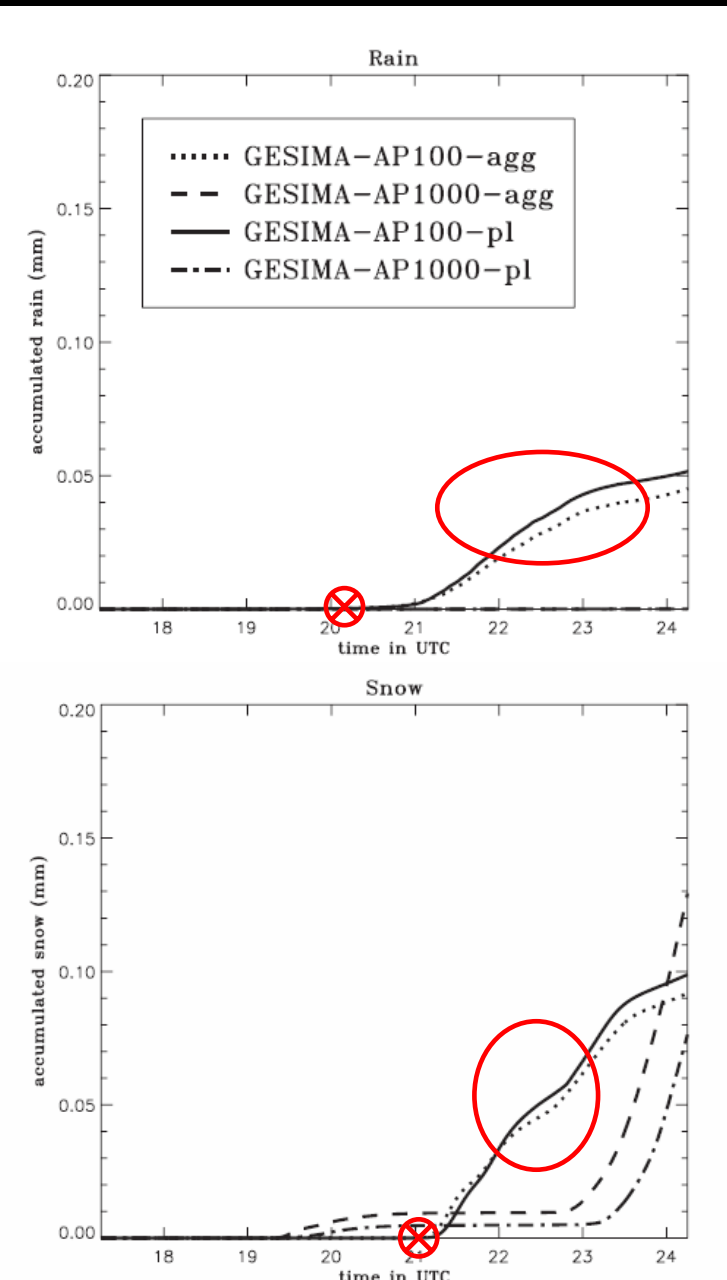
Table 1. Domain Averaged Accumulated Rain and Snow and the Domain- and Time-Averaged Liquid Water Path (LWP), Ice Water Path (IWP), Drizzle Water Path (DWP), and Snow Water Path (SWP)

	Rain, mm	Snow, mm	LWP, g m^{-2}	IWP, g m^{-2}	DWP, g m^{-2}	SWP, g m^{-2}
<i>Planar</i>						
CTL	0.001	0.171	47.6	3.8	0.0	31.2
AP100	0.052	0.099	86.0	3.8	1.6	13.7
AP1000	0	0.076	36.8	3.7	0.0	34.0
AP100-AP1000	0.052	0.023	49.2	0.1	1.6	-20.3
<i>Aggregates</i>						
CTL	0	0.135	37.9	3.9	0.0	28.2
AP100	0.045	0.092	84.8	3.9	1.5	13.7
AP1000	0	0.129	30.2	3.8	0.0	37.5
AP100-AP1000	0.045	-0.037	54.5	0.1	1.5	-23.9

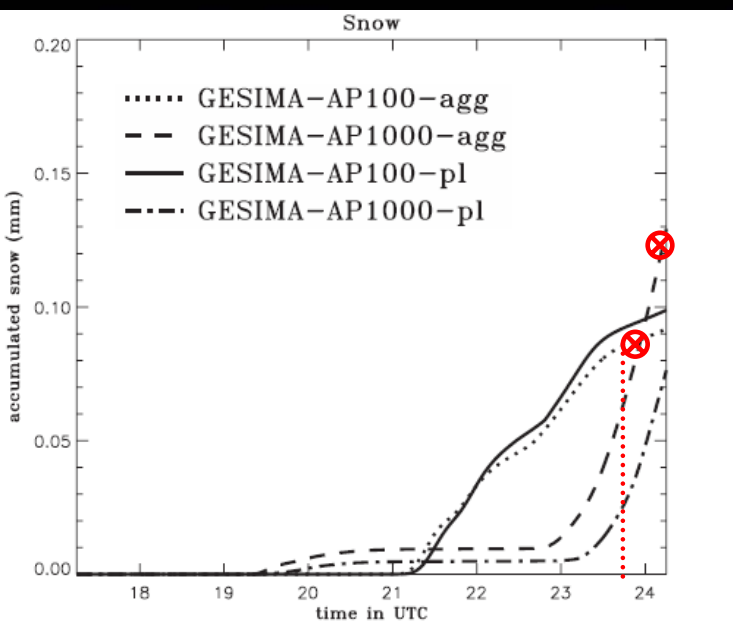


Effect of increased aerosol concentration on Precipitation: autoconversion

The autoconversion rate which depends on the droplet radius, or for the same liquid water content is inversely proportional to the cloud droplet number concentration, is greater for the clean aerosol case compared to the polluted case. Thus more liquid water is converted to drizzle in AP100 as evident after 2000 UTC. The formation of drizzle size drops then enhances their collision with snow flakes that leads to the built-up of snow water path after 2100 UTC



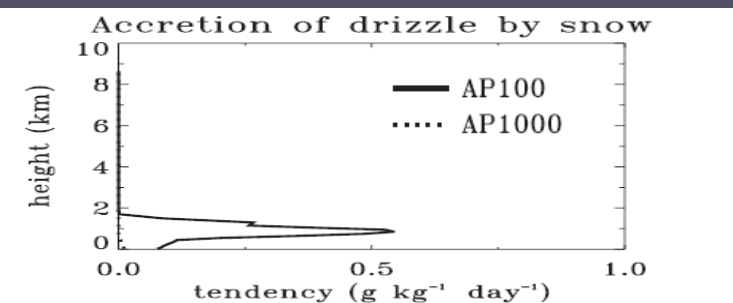
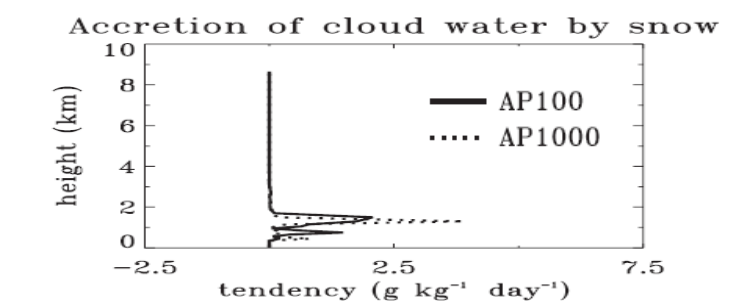
Effect of increased aerosol concentration on Precipitation: accretion of drizzle and cloud droplets by snow



Snow accretes more drizzle in AP100, but more cloud droplets in AP1000. The net effect of these tendencies leads to an overall higher snow in AP1000

In case of aggregates, it takes until 2345UTC before the snowfall rate in AP1000 exceeds that in AP100

In case of planar, the snowfall rate remain larger in AP100 than that in AP1000 during the simulation time



This is caused by the smaller collection efficiency in the polluted cloud for planar crystal compared to the simulation assuming aggregates (That is also the reason why the SWP is smaller and LWP is larger in AP100)

Conclusion

1. Accretion of cloud droplets by snow is increased in polluted cloud due to its higher cloud droplets number concentration; Accretion of drizzle by snow, autoconversion is decreased due to the shutdown of the collision-coalescence process.
2. The precipitation reaching the surface as snow depends on crystal shape: Tenfold increase in aerosol concentration leads to an increase in accumulated snow by 40% for aggregates, but a decrease by 30% for planar crystal.
3. The Total precipitation is decreased for polluted cloud by 7% if it is assumed planar crystal or 50 % if it is assumed aggregates.

Discussion Questions

Both Girard and Lohmann make assumptions about the aerosol's nucleation effect. Are these assumptions reasonable?

In Girard, et al:

based on the observation, vertical uniform

In Lohmann, et al:

parameterization Eq. $N_c = wN_a / (w + cN_a)$

ice crystal formation in the model doesn't depend on the aerosol concentration. Vertical uniform

	Scenario A	Scenario B	Scenario C
Aerosol composition	100% Ammonium sulphate	As observed	100% Sulphuric acid
Homogeneous freezing temperature of haze droplets	Cziczo and Abbatt (1999)	Koop et al. (1998)	Koop et al. (1998)
Ice nuclei (IN) concentration	Meyers et al. (1992) ($F_r=1.$)	Meyers et al. (1992) reduced by a factor F_r ($F_r=108.67^{sw}$)	Meyers et al. (1992) reduced by four orders of magnitude ($F_r=0.0001$)